Journal of Materials and Environmental Sciences
ISSN : 2028-2508

JMES, 2017 Volume 8, Issue 11, Page 4057-4067

http://www.jmaterenvironsci.com

Corrosion inhibition of Cu-30Ni in neutral chloride media polluted by sulphide ions in presence of 2-Mercaptobenzimidazole

M. Benmessaoud[2, 3], A. Al Maofari[1, 3], Y. Nasser Otaifah[3], N. Labjar[4], M. Serghini Idrissi[3], D. Bartout[2], S. El Hajjaji[3]

1. Laboratoire de Physico-chimie, Faculté des Education, Lettre et Sciences, Université d'Amran, Yémen
2. Laboratoire d'Energétique, Matériaux et Environnement-CERNE2D, Ecole Supérieure de Technologie Mohammed V University Rabat, B.P. 227 Salé médina Maroc
3. Laboratoire S3MN2E-CERNE2D, Faculty of Sciences, Mohammed V University Rabat, Av. Ibn Battouta, B.P. 1014, M-10000 Rabat, Morocco
4. Laboratoire S3MN2E-CERNE2D, Procédés et Process Industriels, Mohammed V University Rabat, ENSET, Rabat, Morocco

Received 21 Feb2017,
Revised 08 May 2017,
Accepted 13 May 2017

Keywords

- ✓ Copper-nickel ;
- ✓ Inhibitor;
- ✓ Efficiency;
- ✓ Polarization;
- ✓ Impedance

M Benmessaoud
benmessaoudmma@gmail.com
+212658703826

Abstract

The effect of 2-mercaptobenzimidazole (2-MBI) on the corrosion of Cu-30Ni alloy in NaCl 3% solution polluted by sulphide ions was studied by weight loss measurements, potentiodynamic polarization and impedance spectroscopy (EIS) methods. It is concludes that the presence of sulphide ions in NaCl 3% accelerates the corrosion of Cu-30Ni alloy. To protect the Cu-30Ni alloy structure from the corrosion in presence of sulphide as pollutants, the anticorrosion effect of 2-mercaptobenzimidazole was examined. The obtained results show that 2-MBI acts as a good mixed-type inhibitor retarding the anodic and cathodic reactions. The inhibitory efficiency determined by the electrochemical measurements increases with immersion time.

1. Introduction

According to their good electrical and thermal conductivities, corrosion resistance, and easy useful for the fabrication of equipment, copper and copper-nickel alloys are extensively used in marine applications and in desalination plants [1-6]. Copper nickel has been widely used as tubing material condensers and heat exchangers in various water-cooling systems [7-12]. X. Zhu and al [13] studied the corrosion product films of 70Cu-30Ni alloy in seawater for different durations and the effect of the degree of recrystallization on the characteristics of the corrosion product films; they concluded that the films formed on the recrystallized alloy in seawater were thin, uniform and rich in nickel. However, the presence of certain pollutants such as sulphurs and ammonia compromise their corrosion resistance especially in seawater [14-18]. The presence of sulfide contamination causes serious corrosion if polluted and aerated conditions alternate, or if oxygen and sulfide are simultaneously present [19].

On the other hand, the sulphurs are not dangerous in the absence of oxygen [20]. Other authors [21] investigated the effect of ammonia, they have observed that the presence of ammonia favour the selective corrosion of copper nickel alloys by the formation of complexes compounds with copper. Copper complexes formed with ammonia molecules easily destabilize the layers of corrosion products, which generally protect copper alloys [22]. Many inhibitors have been used to minimize the corrosion of copper and its alloys in different media[23-40].The heterocyclic organic compounds, namely, azoles, were reported to show marked inhibition efficiency [14, 17, 29-35].In previous work [29], the superiority of 2-MBI in a solution of 3%NaCl polluted with ammonia in comparison with other azole compounds, namely Bitriazole and aminotriazole was marked. This superiority was clearly marked in the polarization curves and in the spectra of electrochemical impedances.

The aim of this work is to study the corrosion behaviour of Cu- 30Ni alloy in NaCl 3% solution polluted and unpolluted by sulphide ions in the presence of 2-Mercaptobenzimidazole (2MBI). Weight-loss studies, electrochemical impedance, potentiodynamic polarization, SEM have been used in the present work.

1. Experimental condition

2.1. Materials and solutions

The Cu–Ni alloy used is of commercial grade and has the following composition (wt. %): 69.3 % Cu, 29.6 % Ni, 0.7 % Mn, 0.4 % Fe. The solutions used in this study were prepared of reagent grade chemicals. The standard aggressive medium was NaCl 3%. Sulphides were introduced by the addition of 2 ppm S^{2-} as Na_2S to the NaCl3% solution. 2-MBI used as a corrosion inhibitor was purchasedfromFluka (Scheme 1).

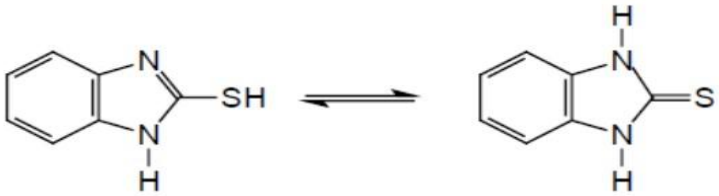

Scheme 1: Chemical structure of 2-Mercptobenzimidazole (2-MBI)

2.2. Methods

2.2.1. Gravimetric measurements

Weight-loss method measurements were performed with rectangular Cu-30Ni coupons (5 cm × 3 cm× 0.3 cm). The coupons were immersed in 300 mL of corrosion solution with and without inhibitors and allowed to for 1 day at room temperature (25°C). Afterwards, the coupons were rinsed with distilled water and adherent corrosion products were removed by immersing the coupons in 6% H_2SO_4 for 20s. Then the coupons were rinsed with distilled water, cleaned with acetone, dried and weighed. Duplicate tests were conducted for each experiment.

The corrosion rate CR and the percentage of inhibition efficiency E_{CR} (%) over the exposure period were calculated using the following equations [41]:

$$CR = 87.6 \times \frac{W}{D \times A \times T} \quad (1)$$

$$E_{CR} = \frac{CR - CR_{inh}}{CR} \times 100 \quad (2)$$

Where A is the area, T the immersion time, W the weight loss and D the density of the specimen.

2.2.2. Electrochemical measurements

For the potentiodynamic polarization experiments, electrochemical cell with a three-electrode configurationwas used. A standard calomel reference electrode (SCE) and a platinum electrode were used as a reference and counter electrodes, respectively. The working electrode was a rotating disk consisting of cylindrical (Cu-30Ni) samples and had a 0,78cm^2 cross-sectional area. The samples were first polished with emery paper grade 1200 and rinsed with distilled water.

The potential polarization studies were carried out using PGZ100 potentiostat. The working electrode was initially immersed in aerated solution at room temperature, and allowed to stabilize for 1 hour at open circuit potential. Then the cathodic and the anodic curves were recorded by changing stepwise (1mv/s) the potential. The rate of rotating electrode is 1000rpm.

The inhibition efficiency were calculated from corrosion current density using the following formula

$$E(\%) = \frac{I_{corr}^0 - I_{corr}}{I_{corr}^0} \times 100 \quad (3)$$

Where I_{corr}^0 and I_{corr} are the corrosion current densities obtained in the absence and presence of the inhibitors, respectively.

Electrochemical impedance spectra (EIS) were carried out at the open-circuit potential E_{corr} using a potentiostat PGZ100with a small amplitude ac signal (10 mV rms), over a frequency range from 100 kHz to 10 mHz with ten points per decade. These tests were performed in the potentiostatic mode at the corrosion potential after 1

hour of immersion time. Data were presented as Nyquist plots. IE % were calculated using the following equation.

$$E_R(\%) = \frac{R_{ct}^i - R_{ct}^0}{R_{ct}^0} \times 100 \qquad (4)$$

where R_{ct}^i and R_{ct}^0 are the charge transfer resistance in the presence and absence of 2-MBI, respectively.

2.2.3. Surface morphology

The surface morphology of the electrode was examined with a scanning electron microscopy (SEM; Leica stereoxam 440). After 24 hours of immersion with and without inhibitor, the specimens were cleaned with double distilled water and dried at room temperature.

2. Results and Discussion

2.1. Gravimetric Measurements

The corrosion of Cu-30Ni alloy in aerated NaCl3% solution, unpolluted and polluted by sulphides, in the absence and in the presence of different concentrations of 2-MBI as inhibitor were investigated by weight loss measurements. The results of gravimetric studies of Cu-30Ni alloy in aerated NaCl3%solution without and with sulphide ions in the absence and presence of two different concentrations of 2-MBI after an immersion period of 5 days are shown in Table 1.

In all corrosive medium, when the concentration of 2-MBI increases, the corrosion rates decrease. The inhibition efficiency of the order of 98% or more is obtained in both polluted NaCl3% solution.

Table 1: Inhibition efficiency for various concentration of 2-MBI for the corrosion of Cu-30Ni alloy in aerated NaCl 3% solution unpolluted and polluted by sulphide ions obtained by weight-loss method

Media	**CR ($\times 10^{-2}$ mmyear^{-1})**	**E_{CR} (%)**
NaCl3%	25.5	-
NaCl3% + 0.5mM MBI	1.56	93.9
NaCl3% + 1mM MBI	1.28	95
NaCl3% + 2 ppm S^{2-}	44.46	-
NaCl3% + 2 ppm S^{2-} + 0.5mM MBI	1.87	95.8
NaCl3% + 2 ppm S^{2-} + 1mM MBI	0.94	97.9

2.2.Open-circuit potential

Figure 1 shows the evolution of the open circuit corrosion potential E_{corr} of Cu-30Ni in 3%NaCl solution unpolluted and polluted by sulphide ions, without and with addition of 1mM 2-MBI.

In absence of inhibitor, it is found that for both corrosive media, the potential of the electrode evolves rapidly towards the positive potentials. After 20 min, the evolution of the corrosion potential becomes slower to reach a quasi-stationary value after 1 hour of immersion time.

In presence of 2-MBI, it is noted that the E_{corr} rapidly stabilizes in the first minutes (10 min), which can be attributed to the adsorption of MTS on the metal surface. E_{corr}shifts slightly towards more positive values for adding of inhibitor.

2.3. Potentiodynamic polarization studies

Cathodic curves of Cu-30Ni alloy in aerated 3%NaCl solution unpolluted and polluted by sulphide ions, without and with addition of 1mM of 2-MBI are shown in Figure 2, Table 2 summarizes the values of associated electrochemical parameters presented in Figure 2. The concentration of 2-MBI is chosen based on the inhibition efficiency obtained from Gravimetric Measurements and from electrochemical studies in the context of a detailed study published elsewhere [30].

In the 3%NaCl solution, the cathodic curves showed a current diffusion plot, which indicates the influence of mass transport. It was previously shown that oxygen reduction is a mixed activation/diffusion process at the corrosion potential [42].

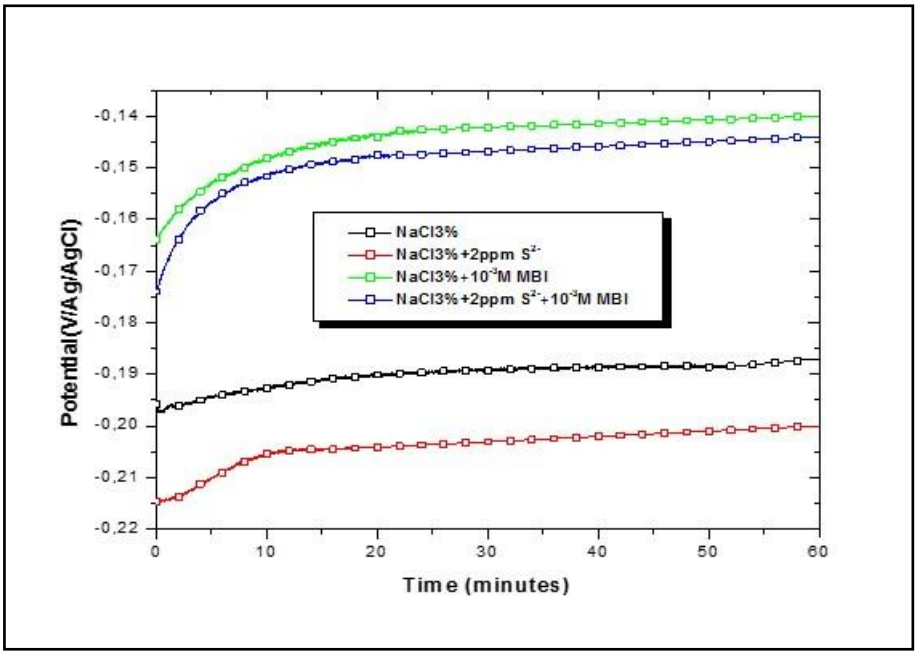

Figure 1: Evolution of Ecorr of Cu-30Ni in 3%NaCl solution unpolluted and polluted by sulphide ions, without and with addition of 1mM 2-MBI at 25°C: Ω = 1000 rpm;

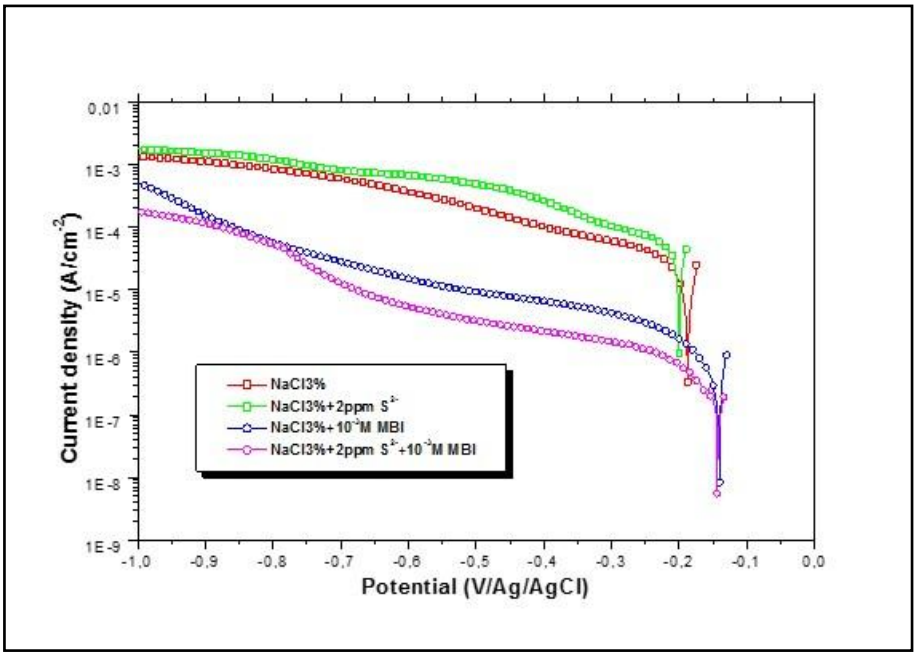

Figure 2: Cathodic polarization curves of Cu-30Ni alloy in aerated 3%NaCl solution unpolluted and polluted by sulphide ions, without and with addition of 1mM 2-MBI at 25°C: Ω = 1000 rpm;|dE/dt| = 1mVs^{-1}

The addition of sulphide ions in the 3%NaCl solution is accompanied by an increase of the current density values near the corrosion potential. This increased from 26.2 µAcm^{-2} without sulphide ions to 47.9 µAcm^{-2} with sulphide ions. The addition of 2 ppm of sulphide ions led to an 83% increase of the corrosion rate (Table 2). In presence of sulphide ions, the cathodic curve showed a shape similar to that obtained in the 3%NaCl solution with a current diffusion plateau characteristic of the transport of dissolved oxygen to the electrode.

On adding 2-MBI to the both corrosive solutions, the corrosion potentials were displacedtowards positive values (Table 2), the cathodic current densities decrease and the control of the cathodic reaction at the corrosion potential is a pure activation.Theinhibition efficiencies reached 96.4% and 99.5% in 3%NaCl solutions without and with sulphide ions at 1mM of MBI respectively.

Table 2. Corrosion inhibition parameters of Cu-30Ni alloy in aerated 3%NaCl solution unpolluted and polluted sulphide ions, without and with addition of 1mM of 2-MBI.

Solution	E_{corr} (mV/Ag-AgCl)	I_{corr} (µA/cm^2)	b_c (mV/dec)	b_a (mV/dec)	E (%)
NaCl 3%	-187	26.2	-258	51	-
NaCl 3% + 1mM 2-MBI	-140	0.94	-217	74	96.4
NaCl 3% + 2ppm S^{2-}	-200	47.9	-247	48	-
NaCl 3% + 2ppm S^{2-} +1mM 2-MBI	-144	0.24	-128	71	99.5

The anodic polarization curves are presented in Figure 3.The addition of sulphide ions in the 3%NaCl is accompanied by an increase of the current density values.Thus at −150 mV, the current density increases from 130µA cm^{-2} without sulphide to 300µA cm^{-2} in the presence of sulphide. This confirms their accelerating effect on the anodic reaction. We note that at the end of the plotted curves, the surface of the alloy is covered with a continuous grey layer in the absence of sulphides. On the other hand, in their presence, the layer is black, porous and non-adherent.

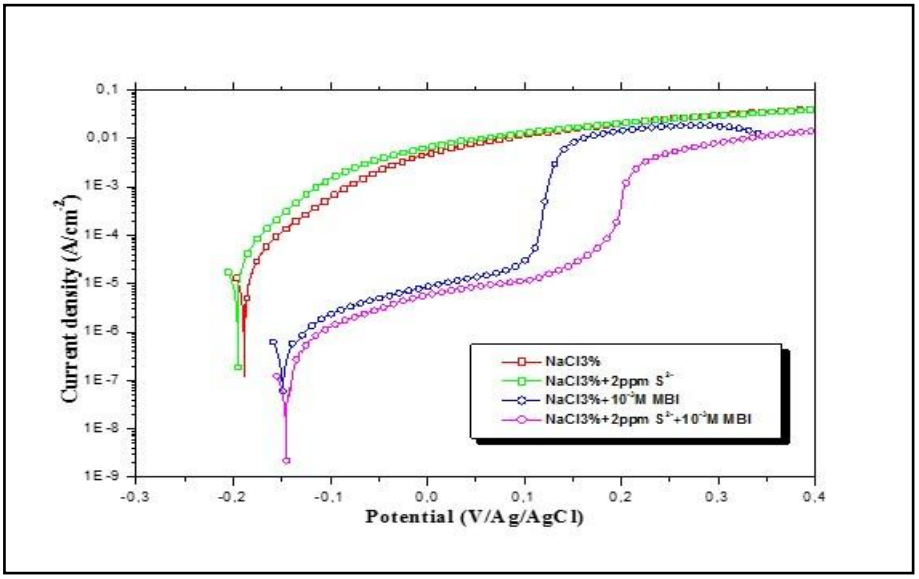

Figure 3: Anodic polarization curves of Cu-30Ni alloy in aerated 3%NaCl solution unpolluted and polluted by sulphide ions, without and with addition of 1mM 2-MBI at 25°C: Ω = 1000 rpm; |dE/dt| = 1mVs^{-1}

The addition of 2-MBI to the all corrosion solutions decreases the rate of alloy dissolution. Anodic polarisation curves presented shows also a change in the shape of polarization curves that may correspond to a likely change in the nature and rate of anodic reaction. These curves show a passive domain, which is clearly observed compared to blank essay. This effect can be explained by the fact that the product tested acts by adsorption on the surface of the material and contributes to an establishment of anodic film formation. This passivity is broken with anodic over tension. This effect can be allotted to the destruction or the desorption of film formed by the 2-MBI on the surface of the electrode.

2.4. Electrochemical impedance spectroscopy

Figure 4presents Nyquist and Bode plots of Cu–30Ni alloy in aerated 3%NaCl solution with and without sulphides ions at corrosion potential (E_{corr}) after 1 h of stabilisation time.

In the absence of sulphides, the Nyquist diagram (figure 4a) presents a flattened semi-circle with a deformation in the high frequency domain. Assuming that two R and C ladder circuits (Figure 5) can describe this impedance data, the impedance spectrum could be fitted suitably. On adding of ions sulphide to the 3%NaCl solution, the impedance diagram changes in shape and size. Though clearly separated, this diagram may be split into two capacitance loops. However, in contrast to the case of copper electrode [43], with Cu-30Ni electrode, the addition of sulphide ions present two capacitive loops and the first loop can be attributed to a charge transfer process. On the same diagrams of figure (4a), the curves adjusted according to the chosen model are plotted. It can be noted that this model describes well the film formed, since the adjusted curves are superimposed well on the experimental curves.

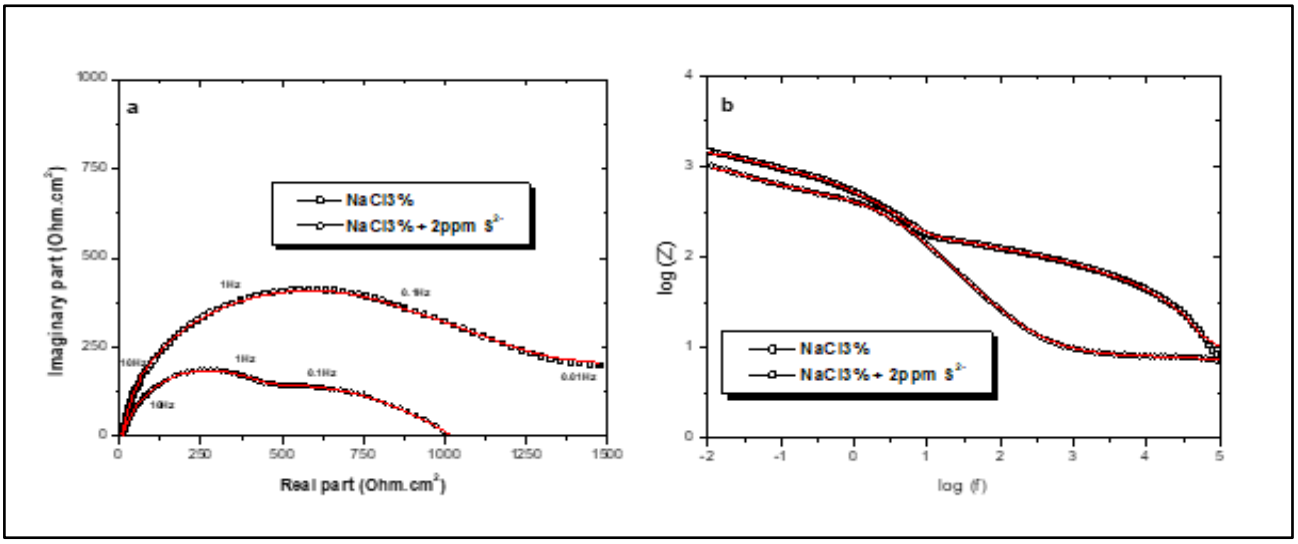

Figure 4:(a) Nyquist and (b) Bode plotsof Cu–30Ni in the corrosion test solution in the absence and presence of sulphides ionsafter 60 min of stabilisation period. Ω = 1000 rpm.

On the same diagrams of figure (4a), the curves adjusted according to the chosen model are plotted. It can be noted that this model describes well the film formed, since the adjusted curves are superimposed well on the experimental curves. In the Bode diagram (figure 4b), and in absence of sulphides, the high frequency part of the curve started from to the origin, indicating a very fast process. The electrical double layer can cause this capacitive behavior. In the low frequency part, we notice a short linear slope and the $\log|Z|$ values still increase and does not reach a constant value as expected, indicating a very slow process (i.e., diffusion limited).

In presence of sulphide ions, we note three distinctive segments. In the high frequency extreme region, the value of $\log|Z|$ tends to become very small. This region is typical of a resistive behaviour and corresponds to solution resistance. In the medium frequency region, a linear relationship exists between $\log|Z|$ and $\log f$. This region corresponds to the charge transfer at the metal/electrical double layer. In the low frequency segment, the resistive behaviour of the electrode increases and the value of $\log|Z|$ should remain constant with a further decrease in frequency. But this behaviour does not reached. $\log|Z|$ still increases, with a decrease in frequency. This corresponds to the diffusion impedance because of the diffusion of oxygen.

The electrical equivalent circuit consists of two parallel R and C proposed in Figure 5, whose components are attributed to: R_{ct}: charge transfer resistance that will be determined essentially by the corrosion process; C_{dl} : double layer capacitance with CPE behaviour, R_F and C_F : Faradaic impedance involving an oxidation–reduction process of the corrosion products.

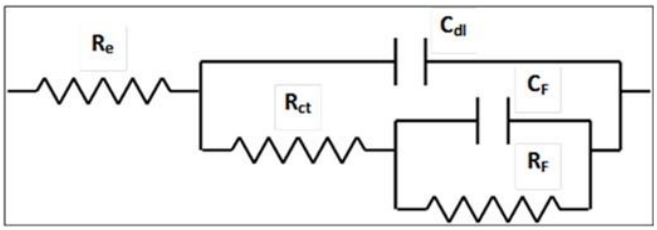

Figure 5: Electrical equivalent circuit used to simulate EIS data for the Cu-30Ni alloy corrosion in 3%NaCl solution without and with sulphides ions.

Nyquist and Bode plots of Cu–30Ni alloy in aerated 3%NaCl solution with and without sulphides ions in presence of 1mM of 2-MBI at corrosion potential (E_{corr}) after 1 h of stabilisation time, are shown in Figure 6a and Figure 6b.

The Nyquist plots show a capacitive behavior of the interface throughout the frequency range examined. The addition of the 2-MBI results in a large increase in the total impedance and a change in the shape and size of the diagrams. According to the variation of the polarization resistance Rp,we note that the polarization resistance increases from 1.5 kΩcm^2 to 70 kΩcm^{2}in 3%NaCl solution and from 1 kΩcm^2 to 90 kΩcm^2 in 3%NaCl polluted by sulphide ions in the presence of 1mM of 2-MBI. That can be interpreted by an effective protection of the metal by the 2-MBI.

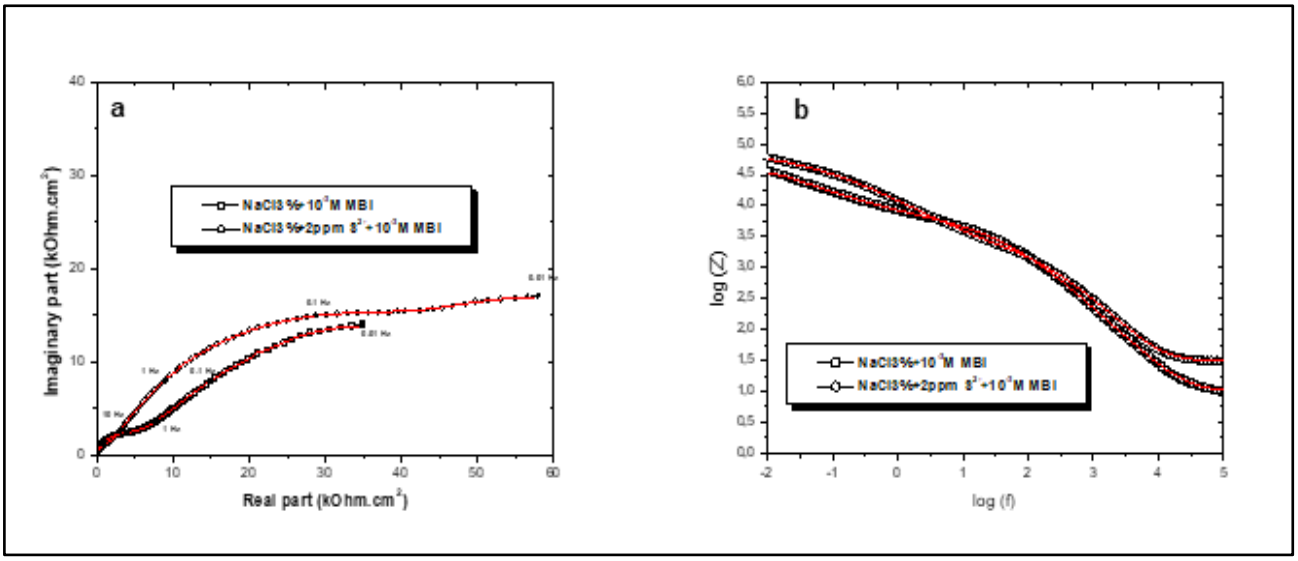

Figure 6:(a) Nyquist and (b) Bode plotsof Cu–30Ni in the various corrosion test solutions in presence of 1mM of 2-MBI after 1 h of stabilisation period. Ω = 1000 rpm.

In the Bode diagrams (figure 6b), the adding of 2-MBI into both corrosives media, leads to a modification on the shape of the diagrams. However, these diagrams may be explained with three R and C circuits. The use of such an electrical equivalent circuit is in agreement with studies detailed elsewhere [44-45].The low frequency capacitive loop CF–RF may be due to a faradaic process involving the surface species issued of corrosion process and metallic species. It may be worth to recall that at the particularly in presence of inhibitor, the diffusion process no longer controls the cathodic reaction. Moreover, the values determined for this couple from the numerical simulations of the ac diagrams are not discussed in the text since it appears that they are scattered probably because they are likely ascribed to corrosion products. The medium frequency contribution is attributed to the double layer capacitance (Cd) at the electrolyte/Cu-30Ni interface at the bottom of the pores coupled with the charge transfer resistance (Rt). The Cd values observed in absence and in presence of 2-MBI are those frequently reported for a flat electrode. In its presence in both corrosives media, the values of Cd is markedly smaller corresponding to the adsorption of inhibitor or the film formation. The Rt value increases markedly when the inhibitor was added to the corrosion tests solutions, which indicates an efficient protective effect of 2-MBI on the corrosion of Cu–30Ni alloy. Whereas, the low frequency elements (Cf–Rf) are ascribed to the dielectric character of the corrosion products (Cf) due to the formation of thin surface film that is reinforced by the presence of the inhibitor and by the ionic conduction through the pores of the film (Rf).
The values determined from a non-linear regression calculation for C_f–R_f and R_{ct}–C_{dl} couples are summarized in Table 3.

Table3. Parameters determined by non-linear regression of the results presented in Figure 4a and Figure 6a

Solution	**C_f (μFcm^{-2})**	**R_f ($k\Omega cm^2$)**	**C_{dl} (μFcm^{-2})**	**R_{ct} ($k\Omega cm^2$)**	**E (%)**
NaCl 3%	-	-	94.40	1.200	-
NaCl 3% + 2-MBI	1.4	5.6	42.90	51.960	97.7
NaCl 3% + 2ppm S^{2-}	-	-	169.5	0.470	-
NaCl 3% + 2ppm S^{2-} + 2-MBI	1.1	2.9	37	54.140	99.1

By analysing the results presented in Table 3, we noted that the value the R_{ct} values, calculated by a non-linear regression, and the inhibiting efficiency increase with 2-MBI. The inhibiting efficiency is evaluated according to the equation (4). The inhibiting efficiency was close to 97.7% and 99.1% when 1mM 2-MBI was added to 3%NaCl solution without and with sulphide ions respectively. The inhibiting efficiency determined by the EIS is close to that evaluated from the cathodic polarization curves.
The capacitance C_{dl} calculated from the characteristic frequency $f_{max}$of the capacitive loop can be attributed to the double layer capacitance, C_{dl}.

Figure 7 and 8 shows Nyquist and Bode plots of Cu–30Ni alloy in aerated 3%NaCl solution with and without sulphides ions in presence of 1mM of 2-MBI at the corrosion potential for different immersion times. It maintains the same shape after 1h of immersion time.

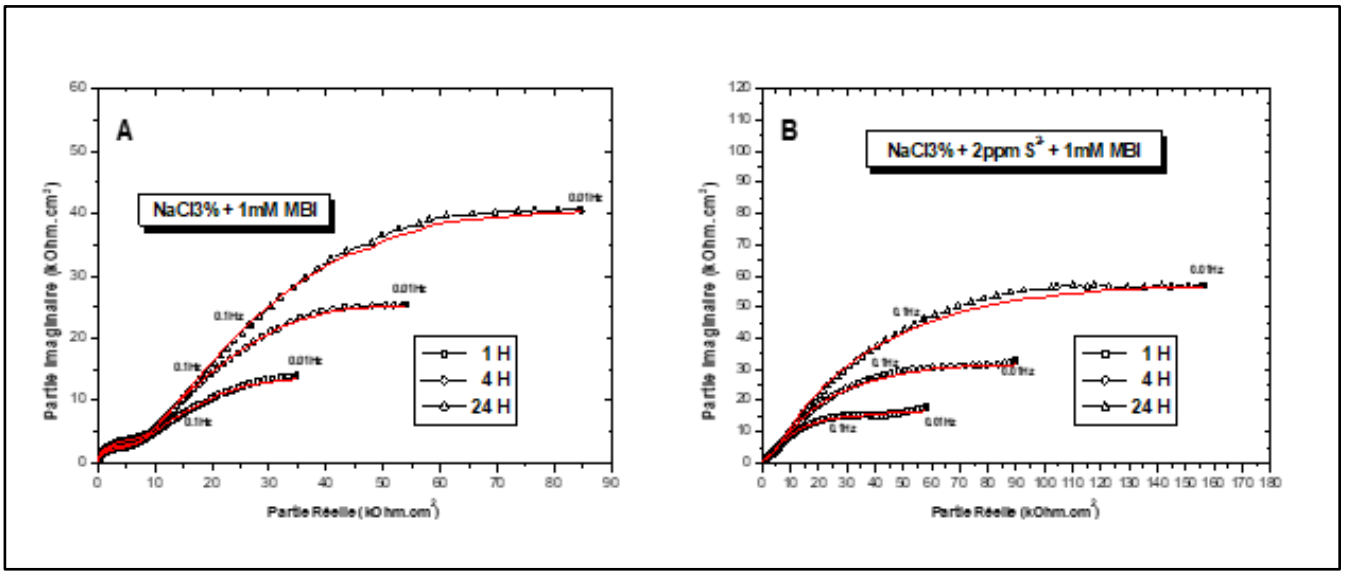

Figure 7: Nyquistplotsof Cu–30Ni in the various corrosion test solutions containing 1mM 2-MBIat various immersion time. Ω = 1000 rpm. (A) 3%NaCl, (B) 3%NaCl+2ppm S^{-2}

As can be seen in figures 7A and 7B, the diagrams in the Nyquist plots becomes larger with time. The increase of the polarization resistance with the immersion period is often reported for the inhibiting action of heterocyclic on copper corrosion [10-12]. The effect of increasing immersion time on impedance spectra is characterized by the increasing size of the two capacitive loops observed, reaching a maximum in 24 h.

Table 4 displays the variation of protective effect of 1 mM 2-MBI added with respect to immersion time for the rotation speed equal to 1000 rpm. The value of the associated capacity was calculated from the relation $C_{dl} = 1/(2\ \pi f R_t)$, where f is the characteristic frequency in the maximum of the loop and $R_t$is the diameter of the capacitive loop associated.

In the whole cases, the protective effectiveness is higher than 99% in presence of sulphide ions. Furthermore, the inhibiting efficiency tends to increase with immersion period. Compared with the solution without sulphide ions, it was observed that protective effect of 2-MBI is reinforced. It is concluded that some synergetic effect is likely to exist between sulphide ions and the 2-MBI molecule.

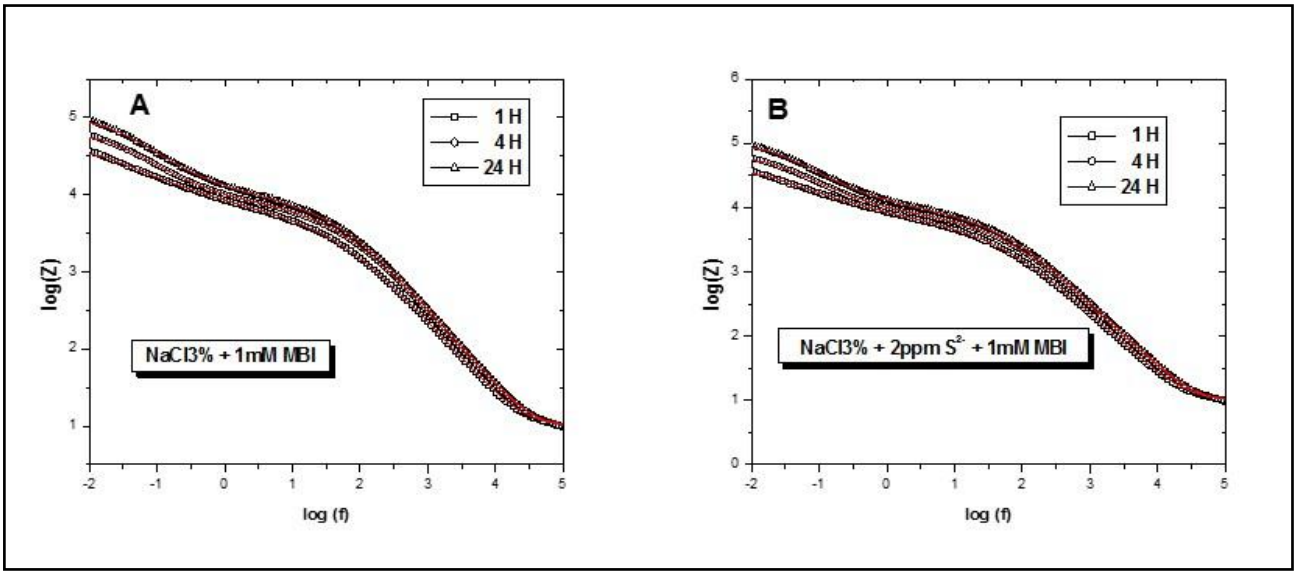

Figure 8: Bode plotsof Cu–30Ni in the various corrosion test solutions containing 1mM 2-MBI at various immersion time. Ω = 1000 rpm. (A) 3%NaCl, (B) 3%NaCl+2ppm S^{-2}

Table4. Parameters determined by non-linear regression of the results presented in Figure 7.

Solution	Time (h)	C_f (μFcm^{-2})	R_f ($k\Omega cm^2$)	C_{dl} (μFcm^{-2})	R_{ct} ($k\Omega cm^2$)	E (%)
NaCl 3%	1	-	-	94.4	1.200	-
	4	-	-	76.2	2.652	-
	24	-	-	72.3	4.400	-
NaCl 3% + 2-MBI	1	1.41	5.64	42.9	51.96	97.7
	4	1	8.88	24.2	65.75	96
	24	0.87	12.95	17.9	88.63	95
NaCl 3% + 2ppm S^{2-}	1	-	-	169.5	0.470	-
	4	-	-	136.8	1.229	-
	24	-	-	118.2	1.346	-
NaCl 3% + 2ppm S^{2-} + 2-MBI	1	1.1	2.94	37.0	54.14	99.13
	4	0.84	3.77	18.5	96.5	98.7
	24	0.66	4.83	14.02	158.9	99.15

2.5.Mechanism of adsorption of 2-Mercaptobenzimidazole

In the context of a detailed study published elsewhere [42], the mechanism of adsorption of MBI on gold and silver surfaces with or without heat treatment has been studied. Indeed, during a simple immersion of these metals in an ethanolic solution, at ambient temperature and without prior heat treatment, adsorption takes place between the sulfur atom and the surface of the materials. On the other hand, when these samples had undergone a heat treatment at 80 ° C for 20 minutes before immersion, the MBI reacts chemically with the silver to form Ag^+MBI^-, while it changes orientation on the gold.

In the case of copper, 2-MBI deprotonates successively in MBI^- and MBI^{2-} [46]. This deprotonation leads to the formation of the MBI^{2-} anion, where the charge is delocalized to the imino group and the other is localized on sulfur.In this case, each metal cation can form a bond with two nitrogen atoms, and then leads to the formation of a polymeric structure. This structure can be attached to the copper surface using the sulfur atom, since each molecule Cu^{2+} MBI^{2-} contains three sites, which allow the formation of these bonds (Figure 9).

2.6.Surface analysis

Figures 10A and 10B present the surface morphology after 24 h of immersion of Cu-30Ni in 3% NaCl solution containing sulphides ions. It can be seen that a continuous grey layer covered the alloy surface after 24h of immersion in NaCl 3% solution. Breakdown of oxide film is also seen.

When 2 ppm of sulfide ions were added to the 3% NaCl solution, the corrosion damage on the alloy surface is relatively more severe. A scale-like black corrosion product covers the entire surface.

However, in presence of 2-MBI in both aggressive media (Figure11A and11B), almost no corrosion is revealed, and the grooves due to the initial surface abrasion remain clearly visible after 24 h immersion. These two micrographs reveals the absence of any corrosion product.

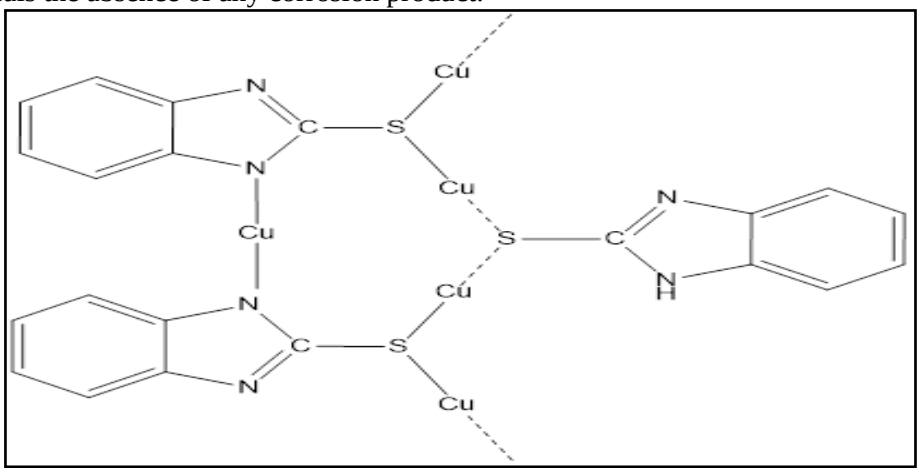

Figure 9: Structure of the Cu-2MBI polymeric film

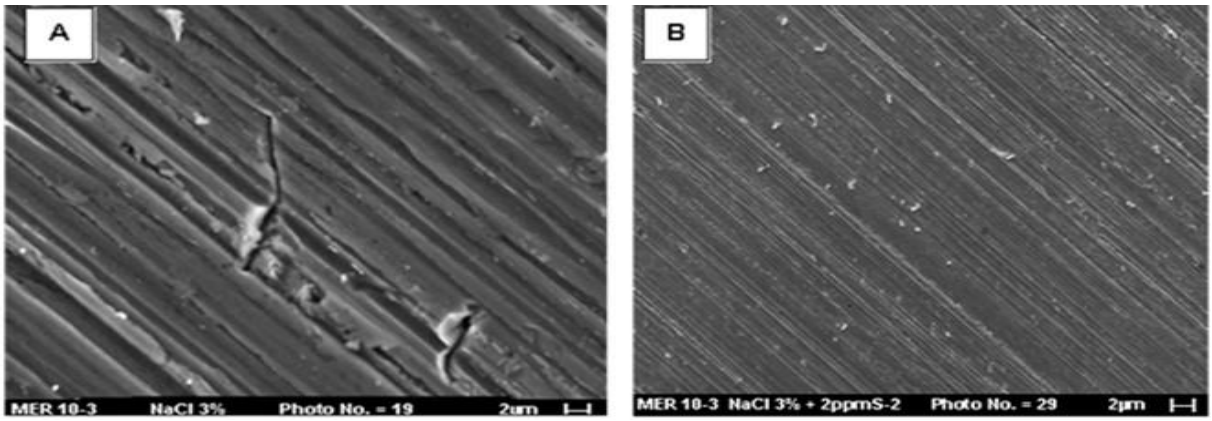

Figure 10: SEM picture of Cu–30Ni electrode surface after 24 h immersion in 3% NaCl in absence (A) and in presence of sulphide ions (B).

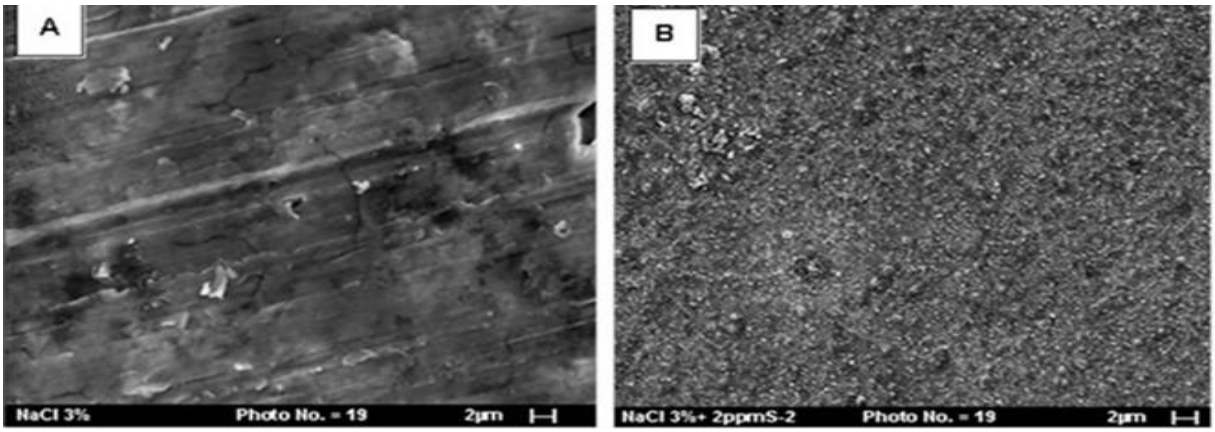

Figure 11: SEM picture of Cu–30Ni electrode surface after 24 h immersion in 3% NaCl in absence (A) and in presence of sulphide ions (B) , in presence of 1mM of 2-MBI

Conclusions

All measurements showed that the 2-Mercaptobenzimidazole has excellent inhibition properties for the corrosion of Cu-30Ni in NaCl3% pure and polluted by sulphide ions. The weight loss measurements show that the inhibition efficiency increases with 2-MBI concentration and reaches its highest values at 1mM concentration. In both corrosive solutions, the potentiodynamic polarisation measurements showed that the 2-MBI inhibits both the cathodic and anodic corrosion processes of alloy, the inhibitions efficiency reaches 96% and 99%. It acts through the establishment of a protective thin film at the surface that prevents the access of oxygen to the metal surface and the transport of reacting species through the film. EIS measurements also indicate that the inhibitor increases the charge transfer resistance and show that the inhibitive performance depends on the formation of thin surface film.

References

1. Cahn R. W., Hassen P., and Kramer E. J., *Mater. Sci. and Technol.*, A Comprehensive Treatment, Structure and Properties of Non-Ferrous Alloys, vol. 8, VCH, New York, NY, USA, (1996).
2. Standards Handbook for Wrought and Cast Copper and Copper Alloy Products; Copper Development Association Inc., New York, (2003)
3. Copper and Copper Alloys Compositions, Application and Properties; Publication 120, Copper Development Association: UK, (2004).
4. John Wiley & Sons., *Uhlig's Corrosion Handbook, Second Edition, Edited by R. Winston Revie*, ISBN 0-471-15777-5, (2000), , Inc. p.729.
5. Sherif M., Erasmus M., and Comins D., *J. Colloid Interf. Sci.*, 311 (2007) 144.
6. Sherif M., Park S., *Electrochim. Acta,* 51 (2006) 4665.
7. North R. F., Pryar M.J., *Corros. Sci.*, 10 (1970) 297.
8. Elmorsi M.A., El sheikh M.Y., Bastweesy A.M., Ghoneim M.M., *B. J. Electrochem*., 7 (1991) 158

9. Osman M., *Mater. Chem. Phy*., 71 (2001) 12.
10. Quraishi M. A., Farooqi I. H., Saini P.A, *Brit. Corros. J.*, 35 (2000) 78
11. Shih H.C., Tzou R.J., *J. Electrochem, Soc*., 138 (1991) 958
12. Quartarone G., Moretti G..Bellami T., *Corros*. 54 (1998) 606.
13. Zhu X., Lei T., *Corros. Sci*., 44 (2002) 67.
14. Es-salah K., Said F., Benmessaoud M., Hajjaji N., Aouial M., Takenouti H., Srhiri A., *Phys. Chem. News*, 23 (2005) 108.
15. Tuck C.D.S., Powell C.A., Nuttall J., *Shreir'sCorros.*, 3 (2010) 1937
16. Ferina S., Loncaret M., Metikos-Hocovic M., Procceding of 8th European Symposium on Corrosion Inhibitors, Ferrara, 1 (1993)1065
17. Laachach A., Srhiri A., Aouial M., Benbachir A., *J. Chim. Phys*., 89 (1992) 201
18. Essom*H., J. Mater. Environ. Sci*.6 (7) (2015) 1850.
19. SherarB.W.A., Keech P.G., Shoesmith D.W., *Corros. Sci.*, 66 (2013) 256.
20. Syrett B.C. et Macdonald D.D., *Corros.*, 35 (1979) 505
21. Francis R., *Brit. Corros. J*., 20 (1985) 167.
22. Jones D. A., "Principles and Prevention of corrosion", Chap.11, Maxwell Macmillan
23. Joseph Raj X. and Rajendran N., *Int. J. Electrochem. Sci*., 6 (2011) 348.
24. Rochdi A., Kassou O., Dkhireche N., Touir R., El Bakri M., EbnTouhami M., Sfaira M., Mernari B., Hammouti B., *Corros. Sci.*, 80 (2014) 442.
25. Hülya K., Süleyman A., *Arab. J. Chem.*, In Press, Corrected Proof, Available online 25 February 2015
26. Damej M., Chebabe D., Benmessaoud M., Dermaj A., Erramli H., HajjajiN.andSrhiri A., *Corros. Eng., Sci. and Techno.*, 50 (2) (2015) 103.
27. Damej M., Benassaoui H., Chebabe D., Benmessaoud M., Erramli H., Dermaj A., Hajjaji N., Srhiri A., *J. Mater. Environ. Sci*., 7 (3) (2016) 738.
28. Benmessaoud M, Serghini-Idrissi M, Labjar N, Rhattas K, Damej M, Hajjaji N, Srhiri A., El Hajjaji S., *Der Pharma Chemica*, , 8(4) (2016) 122.
29. Benmessaoud M., Es-salah K., Kabouri A., Hajjaji N., Takenouti H., Srhiri A., *Mater. Sci. Appl.*, 2 (2011) 276.
30. Benmessaoud M., Es-salah K., Kabouri A., Hajjaji N., Takenouti H., Srhiri A. and Ebentouhami M., *Corros. Sci*., 49 (2007) 3880.
31. Chieb T., Belmokre K., Benmessaoud M., Drissi S-E, Hajjaji N., Srhiri A., *Mater. Sci. and Applic*, 2 (2011) 1260.
32. Appa Rao B.V., Chaitanya Kumar K., *Arab. J. of Chem.*, In Press, Corrected Proof, Available online 9 August 2013
33. Abed Y., Kissi M., Hammouti B., Taleb M., Kertit S., *Prog. Org. Coat*., 50 (2004) 144
34. Dafali A., Hammouti B., Aouniti A., Mokhlisse R., Kertit S., Elkacimi K., *Ann. Chim. Sci. Mat*, 25 (2000) 437
35. Mihit M., El Issami S., Bouklah M., Bazzi L., Hammouti B., Ait Addi E., Salghi R., Kertit S, *Appl. Surf. Sci*. 252 (2006) 2389
36. Badawy Waheed A., Ismail Khaled M., Fathi Ahlam M., *J. Appl. Electrochem*., 35 (2005) 879.
37. Babouri L., Belmokre K., Abdelouas A., Bardeau J.-F., El Mendili Y., *Int. J. Electrochem. Sci*., 10 (2015) 7818.
38. Appa Rao, B.V, Chaitanya Kumar, K. *ISRN Corros.* (2012) 1-22.
39. Fateh A., Aliofkhazraei M., Rezvanian A.R., *Arabian Journal of Chemistry*, (2017) in press.
40. Kovačević N., Milošev I., Kokalj A., Corr. Sci., (2017), in press.
41. Fontana M. G., "Corrosion Engineering," 3rd Edition, McGraw-Hill Book Company, New York, (1987).
42. Laachach A., Srhiri A., Fiaud C.&Benbachir A., *Brit. Corros. J.*, 36 (2) (2001) 292.
43. Rahmouni K., Keddam M., Srhiri A., Takenout H.,*Corros. Sci.* 47 (2005) 3249.
44. Es-Salah K., Keddam M., Rahmouni K., Srhiri A., Takenouti H., *Electroch. Acta*, 49 (2004) 2771.
45. Rahmouni K., Hajjaji N., Keddam K., Srhiri A., Takenouti H..*Electroch. Acta*, 52 (2007) 7519.
46. Assouli B. Etude par émission acoustique associée aux méthodes électrochimiques de la corrosion et de la protection de l'alliage cuivre-zinc (60/40) en milieu neutre et alcalin. Cotutelle Thesis, INSA Lyon University & Kénitra University, December 2002.